

I-8-1

## Self-Assembling Formation of Ni Nanodots on SiO<sub>2</sub> Induced by Remote H<sub>2</sub>-plasma Treatment and Their Electrical Charging Characteristics

K. Makihara, K. Shimanoe, M. Ikeda, S. Higashi and S. Miyazaki

Graduate School of Advanced Sciences of Matter, Hiroshima University  
 Kagamiyama 1-3-1, Higashi-Hiroshima 739-8530, Japan  
 Phone: +81-824-24-7648, FAX: +81-824-22-7038, E-mail: [semicon@hiroshima-u.ac.jp](mailto:semicon@hiroshima-u.ac.jp)

### 1. Introduction

Charge storage in metal nanodots embedded into dielectric layers has received much attention because superior charge retention to semiconductor nanodots can be expected for metals with proper work functions [1]. For the nonvolatile memory application, the formation control of metal nanodots with good size uniformity and an areal density as high as  $\sim 10^{12} \text{ cm}^{-2}$  in gate dielectrics is a crucial issue. So far, metal nanodots, including Au, Ag, Pt, W [2, 3] and Ni [4] have been applied to a floating gate in nonvolatile memories. To settle reliability issues, minimizing the thermal budget is of great importance because metal diffusion often occurs through the oxide [5].

In this work, we have demonstrated a new fabrication method of nanometer-scale Ni dots on SiO<sub>2</sub> from ultrathin Ni films by exposure to a remote hydrogen plasma. Electron charging to and discharging from the Ni nanodots have been studied by a AFM probe technique to confirm the electrical isolation among Ni nanodots.

### 2. Experimental

~3nm-thick SiO<sub>2</sub> was thermally-grown on p-Si(100) and treated by a dilute HF solution to terminate the surface with OH bonds. A ~1.3nm-thick Ni film was evaporated on the SiO<sub>2</sub> by electron beam without any extra heating. Subsequently, Ni films were exposed to a remote plasma of pure H<sub>2</sub> as schematically illustrated in Fig. 1. The plasma was generated in a quartz tube with a size of 10cm in diameter by inductively-coupling with an external single-turn antenna connected to 60MHz generator through a matching circuit. The substrate was placed on the susceptor at a distance of 32 cm away from the position of the antenna to minimize ion damages. For the remote H<sub>2</sub> plasma treatment, gas pressure and VHF power were changed in the range from 0.1 to 0.6Torr and 100 to 350W, respectively, at room temperature. The exposure time to the remote H<sub>2</sub> plasma was kept constant at 5min. The dot density and size uniformity were evaluated by Atomic force

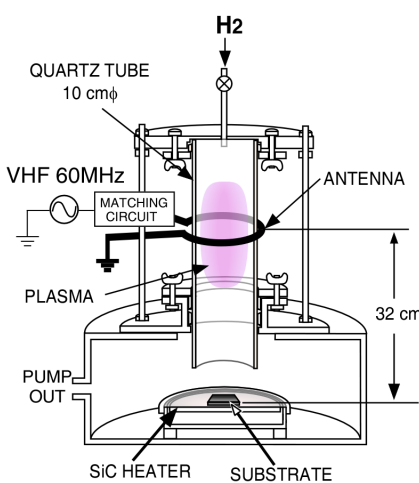


Fig. 1. Schematic view of the remote H<sub>2</sub> plasma treatment equipment.

microscopy (AFM). Also, Electron charging to and discharging from Ni nanodots so-prepared were carried out by scanning the sample surface with an electrically-biased AFM probe tip in a tapping mode at room temperature in clean room air, where a Rh-coated Si<sub>3</sub>N<sub>4</sub> cantilever with a radius of tip apex of ~100nm was used. Before and after electron charging or discharging, the topographic and corresponding surface potential images were simultaneously taken with a non-contact Kelvin-probe mode.

### 3. Results and Discussion

AFM images for as-evaporated Ni films show a fairly smooth surface morphology with a root-mean-square roughness of 0.16nm and are almost identical to those for as-grown SiO<sub>2</sub> surface as shown in Fig. 2. By exposing the Ni films to the remote H<sub>2</sub> plasma under a gas pressure of 0.26 Torr with VHF powers of 350W at room temperature, the formation of Ni dots with an areal dot density of  $\sim 6.7 \times 10^{11} \text{ cm}^{-2}$  and an average dot height of  $\sim 2.0 \text{ nm}$  was clearly observed (Fig. 2(c)). It is likely that surface migration of Ni atoms is induced by atomic hydrogen and results in agglomeration with cohesive action. H<sub>2</sub> pressure dependence of Ni nanodot density at a VHF power of 350W is shown in Fig. 3. With decreasing the H<sub>2</sub> pressure down to 0.1 from 0.26 Torr, the dot density is decreased to  $6.7 \times 10^{11}$  from  $6.5 \times 10^{10} \text{ cm}^{-2}$ , and the increase in the pressure from 0.26 to 0.6 Torr causes a reduction in the dot density down to  $8 \times 10^8 \text{ cm}^{-2}$ . In the pressure region below 0.26 Torr, the generation of atomic hydrogen is likely to limit the dot nucleation density. The reduction of the dot density over 0.26 Torr suggests diffusion loss of atomic hydrogen before reaching the sample surface due to the increased collisions in gas phase. We have also evaluated the effect of VHF power on the dot density as represented in Fig. 4. In the case of remote H<sub>2</sub> plasma treatment with a VHF power of 100W, the Ni dot density was as low as  $5.6 \times 10^9 \text{ cm}^{-2}$ . By changing VHF power

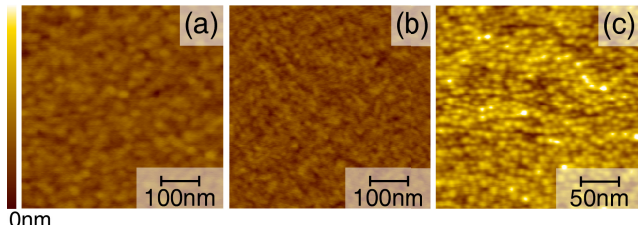


Fig. 2. AFM images of the as-grown SiO<sub>2</sub>(a), ultrathin Ni film deposited on HF-last SiO<sub>2</sub> (b) and Ni film exposed to remote H<sub>2</sub>-plasma with VHF power of 350W (c). The H<sub>2</sub> pressure and substrate temperature were maintained at 0.26Torr and RT, respectively.

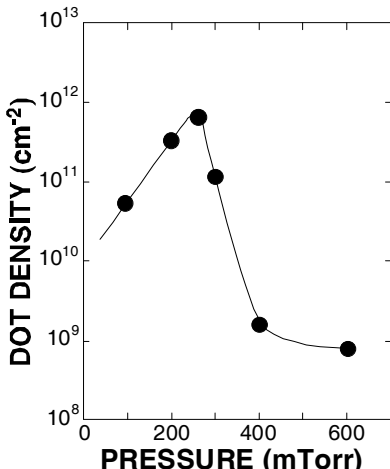


Fig. 3. The areal density of Ni dots formed by the remote H<sub>2</sub> plasma treatment at room temperature as a function of H<sub>2</sub> gas pressure. The VHF power in H<sub>2</sub> plasma generation was kept constant at 350W.

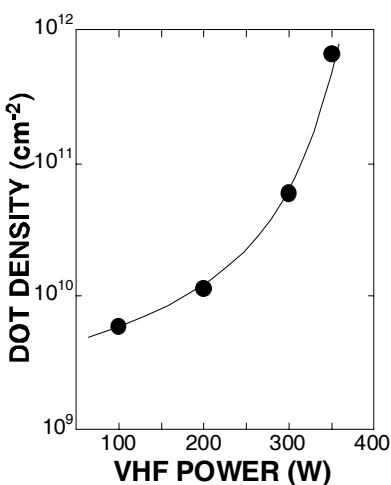


Fig. 4. The areal density of Ni dots formed by the remote H<sub>2</sub> plasma treatment at room temperature as a function of VHF power. The H<sub>2</sub> gas pressure during H<sub>2</sub> plasma treatment was maintained at 0.26Torr.

from 100 to 350W, the Ni dot density is markedly increased by a factor of 13.

To confirm electrical isolation among Ni nanodots so prepared, the surface potential changes due to electron injection to and extraction from Ni dots with ~2nm in height and an areal dots density as high as  $6 \times 10^{11} \text{ cm}^{-2}$  have been studied as shown in Fig. 5. When the surface is scanned with the AFM tip biased at -0.5V with respect to the substrate in the tapping mode, a distinct decrease in the surface potential of corresponding area, which is associated with electron injection to the dot, is observed but, in the unbiased area, no change in the surface potential is detectable. Subsequently by scanning with the tip biased at +0.5V in the central part of electron pre-injected region, the surface potential raises by almost double the change caused in electron injection, which makes the reverse contrast in the surface potential image as shown in Fig. 5 (b) and (c), indicating that Ni nanodots are separated electrically each other. No change in topographic images with electron injection and extraction was confirmed. The changes in the surface potential evaluated from surface potential images after applied various tip biases were summarized in Fig. 6. The tip bias dependence of surface potential change in a stepwise manner confirms multistep electron charging and discharging characteristics of Ni nanodots associated with the charging energy of Ni dot. Notice that, positively charged states occur even at a tip bias of 0V, which can be interpreted in terms of the work function difference between Ni and Rh.

### Summary

The formation of Ni nanodots by the remote H<sub>2</sub> plasma treatment of ultrathin Ni films deposited on SiO<sub>2</sub> has been successfully demonstrated at room temperature. The Ni nanodot density can be controlled in the range from  $10^9$  to  $10^{12} \text{ cm}^{-2}$  by changing the VHF power, the H<sub>2</sub> plasma pressure and the substrate temperature. This technique is very promising for low temperature fabrication of

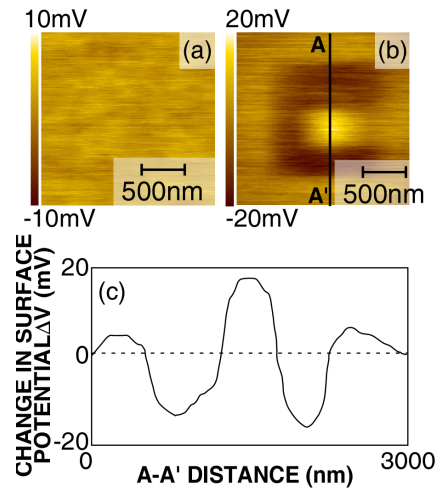


Fig. 5. Surface potential image measured by the Kelvin probe mode before (a) and after electron injection at a tip bias of -0.5V, after electron extraction from the electron pre-injected area at a tip bias of +0.5V (b), one-dimensional potential profile along the line A-A' (c).

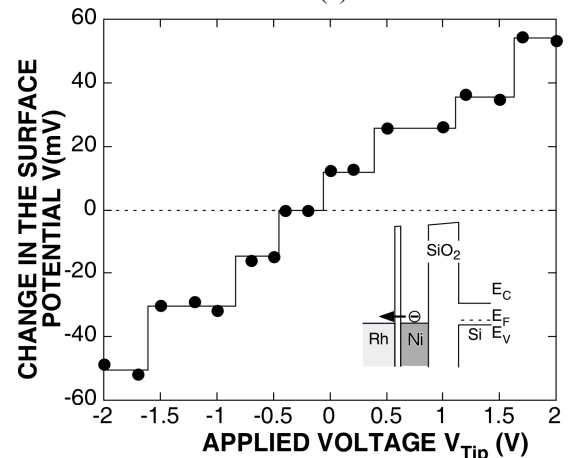


Fig. 6. Surface potential changes caused by electron extraction from and injection to the Ni dots as a function of applied tip bias. Energy band diagram was schematically illustrated in the inset which shows an electron extraction from the dots to the Rh tip at zero bias.

metal-based dots acting as charge storage nodes on the SiO<sub>2</sub>

### Acknowledgement

This work was supported in part by Grant-in Aids for Scientific Research (A) No. 18206035 and for Scientific Research on Priority Area (458) No. 18063017 of MEXT, Japan.

### References

- [1] H. Kirimura et al., Appl. Phys. Lett., 86 (2005) 262106.
- [2] Z. Liu et al., IEEE Trans. Electron Dev. 49 (2002) 1606.
- [3] C. H. Lee, et al., J. Electron Mater. 34 (2005) 1.
- [4] J. J. Lee et al., IEEE Trans. Electron Dev. 52 (2005) 507.
- [5] J. T. Mayer et al., Surface Science 265 (1992) 102.